Preprints of the 18th IFAC World Congress
Milano (Italy) August 28 - September 2, 2011

Autonomous Navigation System of Crawler-Type Robot Tractor

Ryosuke TAKAI*, Oscar BARAWID Jr., Noboru NOGUCHI*****

**Laboratory of Vehicle Robotics, Graduate School of Agriculture, Hokkaido University, Sapporo, Japan (Tel: +81-11-706-3884, Email: takai@bpe.agr.hokudai.ac.jp)*
***Laboratory of Vehicle Robotics, Graduate School of Agriculture, Hokkaido University, Sapporo, Japan (Tel: +81-11-706-3884, Email: oscar@bpe.agr.hokudai.ac.jp)*
****Laboratory of Vehicle Robotics, Graduate School of Agriculture, Hokkaido University, Sapporo, Japan (Tel: +81-11-706-3847, Email: noguchi@bpe.agr.hokudai.ac.jp)*

Abstract: The objective of this research was to modify a commercial crawler-type tractor into a robot tractor that can be navigated autonomously by using RTK-GPS and IMU as navigation sensors. Navigation algorithms were developed. Steering control test and autonomous navigation test in farmland were conducted. Steering control test was conducted in different speeds, and the accuracy was evaluated. In each speed, the robot ran with 1~3cm lateral error. Autonomous navigation test was conducted on multi-path map. In headland area, the robot used keyhole turning and transferred to the next path. The robot could finish the multipath navigation successfully.

Keywords: RTK-GPS, IMU, crawler-type tractor, steering control, keyhole turning, robot tractor

1. INTRODUCTION

Hokkaido, the northernmost island of Japan, is central region of agricultural industry in Japan, in spite of its long time winter season and accumulated snow. Hokkaido prefecture has about 83,456 km^2 land area, which occupies about 22% of Japanese land. Its rich and broad plain fields and primal acceptance of large-scale agricultural production system enabled Hokkaido to become Japan`s capital production area of wheat, paddy, corn, potato, dairy cattle, and so on. Though Hokkaido is such a capital area of agriculture, the shortage of agricultural work force and its aging farmers is happening.

A crawler-type tractor is a vehicle with tracks instead of wheels. Crawler-type tractors are widely used in Japan, especially in paddy fields, because of their high traction and low ground pressure. And they are also used on purpose for snow removal in the winter season. Crawler-type tractors are different from wheel-type tractors in their steering control mechanisms. The tractor controls its direction by changing the rotation velocity between the two crawlers. The two crawlers can spin in the counter direction each other. So it can turn in small radius and even on the spot.

Fig.1. CT801 (YANMAR)

The objective of this research was to develop a crawler-type robot tractor that works in agricultural fields. The authors modified a commercial crawler-type tractor into robot tractor based on RTK-GPS (Real-time kinematic global positioning system) and IMU (Inertial measurement unit) as navigation sensors.

2. MATERIALS AND METHODS

2.1. Research platform and navigation sensors

Table.1. Specifications of a crawler tractor

Model		CT801
Drive system		Crawler
Dimensions		
	Overall length,mm	3750
	Overall width,mm	1950
	Overall height,mm	2635
	Ground clearance,mm	380
Weight	kg	3990
Engine		
	Model	4TNV98T
	Type	4-cycle, water-cooled diesel
	Output(kw(ps))	58.8(80)
	Disppacement(cc)	3318
	Fuel Tank Capacity(lit)	150
Crawler Track		
	Length(mm)	2165
	Width(mm)	450
	Tread(mm)	1500
	Brake	Wet disk
	Max, travel speed (km/hr)	
	Front	18
	Rear	18

Fig.2. RTK-GPS (Legacy-E TOPCON) antenna and receiver

Fig.3. IMU (Inertial measurement unit)

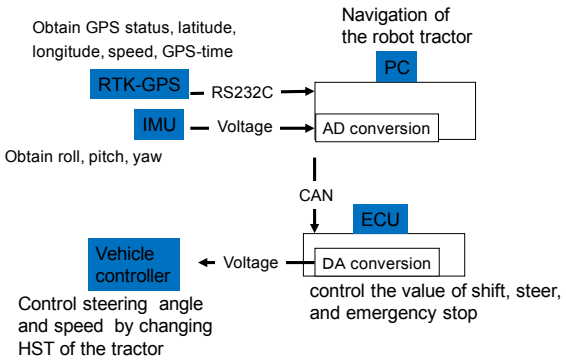

Fig.4. Schematic diagram of a robot tractor

Figure 1 shows the research platform, A YANMAR CT801, acrawler-type standard tractor was used in this research. Table.1 shows its specification. Table 1 shows specification of YANMAR CT801. It has about 4,000 kg weights and engine output is 80ps. Figure 2 shows schematic diagram of the robot tractor. RTK-GPS and IMU were used as navigation sensors to determine lateral and heading errors which were necessary in to evaluate the autonomous navigations. Figure 3 shows the RTK-GPS's (Legacy-E, TOPCON) antenna and receiver. To obtain the absolute position of the robot vehicle, a VRS (Virtual reference station) was used with positioning accuracy of ±2 cm. Fig.4 shows IMU (Inertial measurement unit) (JCS-7401A, Japan Aviation Electronics Ind., Ltd.) used as the posture sensor that could obtain roll, pitch and yaw, and angular velocity of the robot vehicle. It could measure roll and pitch angles within ±45° and yaw angle of ±180°. The IMU has a drift error of 0.5deg/hour. The error was corrected dynamically using sensor fusion algorithm based on IMU and GPS signal.

Control PC in the vehicle calculated vehicle's functions for autonomous navigation using developed algorithms and navigation maps. ECU (Electrical control unit) was developed to convert control PC's digital signal to analog signal to operate the vehicle. ECU has the CAN (Control area network) bus interface and communicated with the control PC. ECU sent analog signals to vehicle's actuators.

Vehicle's functions, forward and backward movement, steering angle, height of three-point link hitch, engine speed, PTO`s turning on and off, were controlled by ECU.

2.2 Sensor fusion

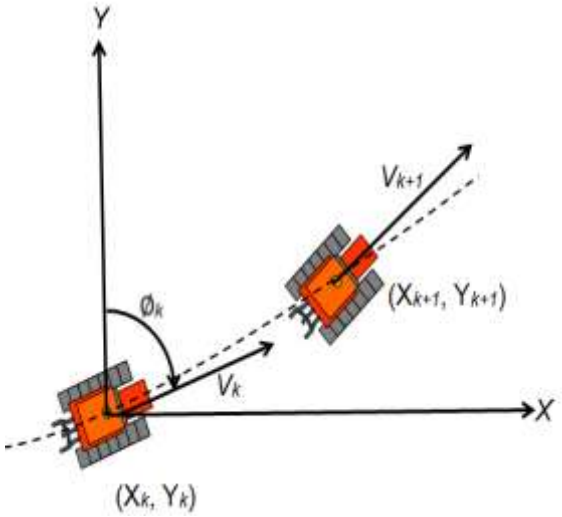

Fig.5. Vehicle dynamics model using RTK-GPS and IMU for sensor fusion

To obtain the lateral error direction of the robot vehicle, an LSM (Least square method) was used (Kise 2003). Figure 5 shows the vehicle dynamics using the RTK-GPS and IMU sensor fusion.

The robot vehicle's absolute position (X_{k+1}, Y_{k+1}) can be calculated using (1) and (2).

$$X_{k+1} = X_k + \int_k^{k+1} V(t)\sin\emptyset(t)\,dt \approx X_k + \frac{1}{2}V_k\Delta t(sin\emptyset_k + sin\emptyset_{k+1}) \quad (1)$$

$$Y_{k+1} = Y_k + \int_k^{k+1} V(t)\cos\emptyset(t)\,dt \approx X_k + \frac{1}{2}V_k\Delta t(cos\emptyset_k + cos\emptyset_{k+1}) \quad (2)$$

Where:

X_{k+1}, Y_{k+1} = absolute position of the vehicle, m

V_k = travel speed, m/s

ϕ_k = absolute heading direction of the vehicle, deg

t = time, sec

The absolute heading direction of the robot vehicle can be calculated using (3).

$$\phi_k = \phi_{IMU_k} + D_k \quad (3)$$

Where:

ϕ_k = absolute heading direction, deg

ϕ_{IMU_k} = relative angle measured by the IMU, deg

D_k = correction value which compensates the drift error, deg

The vector of the vehicle position can be calculated using (4) and (5)

$$e_{P_k} = \begin{pmatrix} X_{k+1} - X_k \\ Y_{k+1} - Y_k \end{pmatrix} \quad (4)$$

$$e_{\emptyset_k} = \frac{V_k \Delta t}{2} \begin{pmatrix} sin\emptyset_k + sin\emptyset_{k+1} \\ cos\emptyset_k + cos\emptyset_{k+1} \end{pmatrix} \quad (5)$$

Evaluation function to decide D_k was defined as (6).

$$I_k = \sum_{i=k-N}^{k} \left\| e_{P_{i-1}} - e_{\emptyset_{i-1}} \right\|^2 \quad (6)$$

Since I_k is sum of the error, a proper D_k can be calculated by using (7) that minimizes the I_k

$$\frac{dI_k}{dD_k} = 0 \quad (7)$$

Where:

N=number of navigation points

e_{P_k} = vector of the vehicle position by position sensor

$e_{\emptyset_k}$=vector of the vehicle position by posture sensor and velocity sensor

(8) can be described from (1) to (6)

$$I_k = \sum_{i=k-N}^{k} \{dX_i^2 + dY_i^2 + S_i^2 + C_i^2 - 2(dX_i S_i + dY_i C_i) cos D_k + 2(-dX_i C_i + dY_i S_i) sin D_k\} \quad (8)$$

Where:

$$dX_i = X_i - X_{i-1} \quad (9)$$

$$dY_i = Y_i - Y_{i-1} \quad (10)$$

$$S_i = \frac{1}{2} V_i \Delta t (\sin\emptyset_{IMU_i} + \sin\emptyset_{IMU_{i-1}}) \quad (11)$$

$$C_i = \frac{1}{2} V_i \Delta t (\cos\emptyset_{IMU_i} + cos\emptyset_{IMU_{i-1}}) \quad (12)$$

Finally,

D_k is calculated using (7) and (8).

$$D_k = tan^{-1}\left(\frac{\sum_{i=k-N}^{k}(dX_i C_i - dY_i S_i)}{\sum_{i=k-N}^{k}(dX_i S_i + dY_i C_i)}\right) \quad (k > N)$$

$$D_k = tan^{-1}\left(\frac{\sum_{i=0}^{k}(dX_i C_i - dY_i S_i)}{\sum_{i=0}^{k}(dX_i S_i + dY_i C_i)}\right) \quad (k \le N) \quad (13)$$

2.3. Navigation map

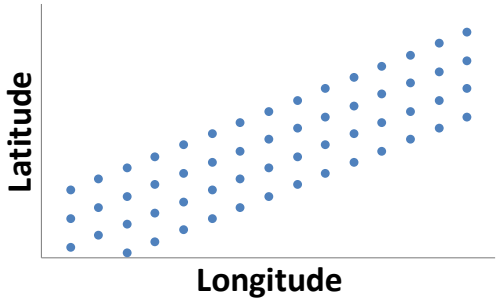

Fig.6. Navigation map

Figure 6 shows the straight lines composed of three dimensional points which were created by GIS. The robot works following the navigation map. Navigation points were defined as three dimensional Euclidean space E^3 shown as (14) (Kise 2003).

$$\Omega = \{\omega_i | \omega_i \in E^3, 0 < i \le N\}$$

$$\omega_i = (lat_i, lon_i, code_i) \quad (14)$$

Where:

ω_i: Navigation points

N: The number of navigation points

lat_i, lon_i: Latitude and longitude of navigation points in WGS-84 coordinate

$code_i$: Codes of vehicle`s jobs.

2.4. Steering control algorithm

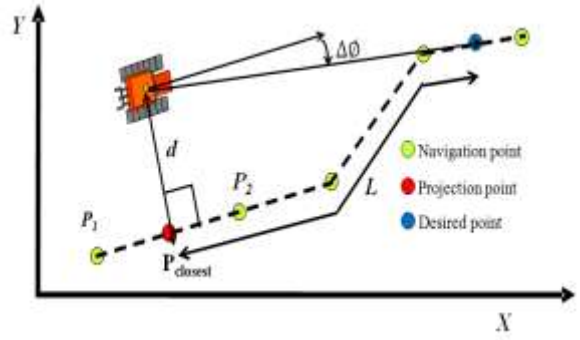

Fig.7. Steering control

The robot changes its steering angle dynamically on the straight lines of navigation map. Steering angle δ was calculated using PID control based on lateral error d and heading error Δ∅ shown as (15). Figure 7 shows the algorithm of steering control.

$$\delta = a_1 d + a_2 \Delta\emptyset \quad (15)$$

2.5 *Keyhole turning*

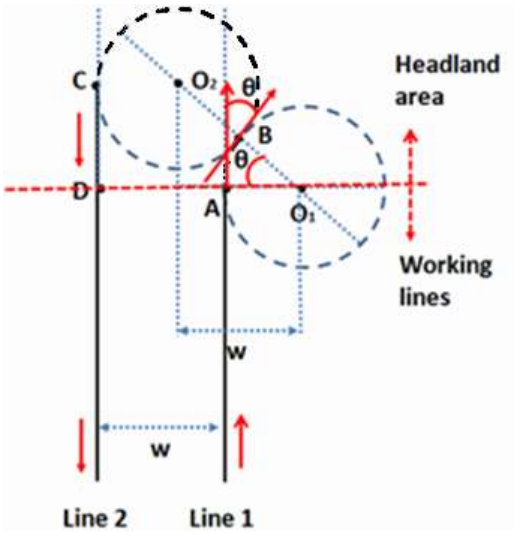

Fig.8. Schematic trajectory of keyhole turning

After the robot finishing a path, it turns in the headland to enter the next path. Keyhole turning is a way of turning that contains no backward movements. Diagram of a keyhole turning is shown in Fig.8.

During this turning, the robot tractor turns in the same radius, so the influence on the ground is thought to be almost constant. The radius can be changed by the ground condition. In this figure, vehicle advances on point-A, point-B, point-C, point-D, in order. Equation (4) was used to represent θ.

$$\theta = cos^{-1}(w/2 * r) \quad (4)$$

Where:

θ: turning angle from point-A to point-B

w: width between two working lines

r: turning radius

2.6. *Autonomous navigation tests*

Automatic navigation tests were conducted on single-line path and multiline paths. At first, single-line path navigation test was conducted on a road in fields to test the accuracy of steering control. The robot followed the line using algorithm shown in (3) and Fig.3 in different speeds. The gains were changed as to the speed. In each speed, the accuracy was evaluated as lateral and heading errors. Then autonomous navigation test was conducted. Four path lines were created by GIS, and in headland area the robot turned with keyhole turning that used algorithm shown in (4) and Fig.4. The speed was about 1m/s on straight lines and about 0.4m/s during headland turning. Acceleration speed, PTO and the height of three-point hitch were also controlled in this navigation. On path lines, acceleration speed were elevated, PTO rotated and three-point hitch was moved downward. During turning, acceleration speed was reduced, PTO stopped and three-point hitch was moved upward.

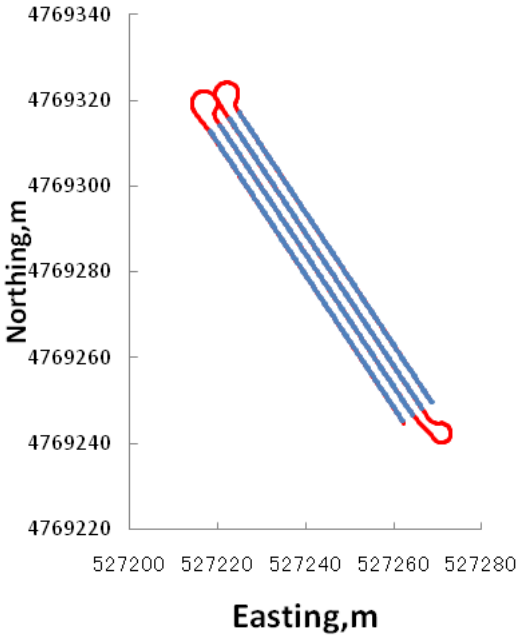

Fig.9. Trajectry of autonomous navigation

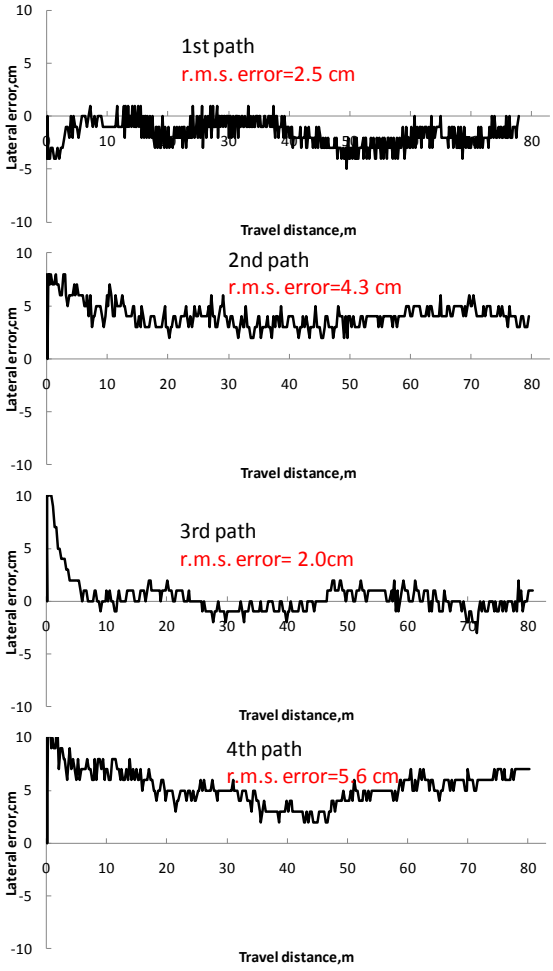

Fig.10. Lateral error of autonomous navigation

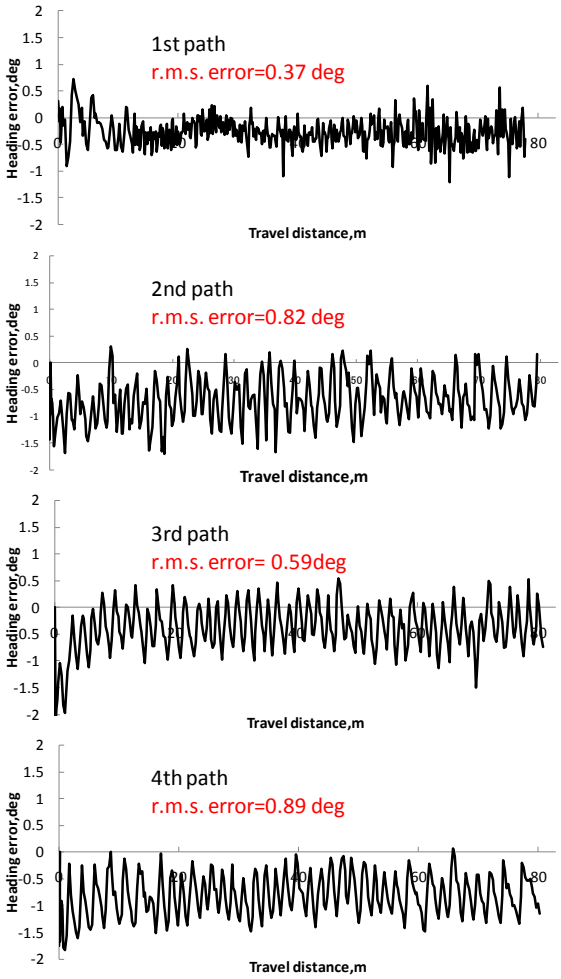

Fig.11. Heading error of autonomous navigation

Table.2. Accuracy of straight line navigation

Speed,m/s	r.m.s lateral error,mm	r.m.s heading error,deg
0.6	10	0.24
0.9	18	0.47
1.3	29	0.76
1.7	22.3	0.63
2	18	0.54

3. RESULTS AND DISCUSSION

Table 2 shows the RMS lateral and heading error of single path navigation test in each speed. The lateral error was about 1~3 cm and the heading error was less than 1 deg. This result suggested the robot has enough accuracy to satisfy automatic navigation in a speed less than 2m/s. Figure 9 shows the trajectory of multipath navigation. The robot followed the navigation map and worked its jobs on straight lines. In headlands, the robot turned using keyhole turning algorithm and entered to next path with 4~10 cm errors. Figure 10 and 11 shows the transition of lateral and heading error respectively. The lateral error at the beginning point of each path was converged gradually.

4. CONCLUSION

The authors modified a standard crawler-type tractor into a robot tractor that controls functions electrically and navigates itself automatically following a navigation map. Navigation map was created by the GIS. Steering control algorithm and keyhole turning algorithm was developed and autonomous navigation tests were conducted. On a single straight line path, the robot ran with 1~3cm lateral error and less than 1 deg heading error at the speed of 0.6~2 m/s. This result suggested that this agricultural robot had enough ability to work on straight lines at the speed less than 2 m/s. On multiline path, the robot controlled its functions such as speed, steering angle, PTO, tree-point hitch, and in headland area, it turned with keyhole turning. The robot finished its autonomous navigation successfully.

REFERENCES

Noguchi, N., Ishii, K., and Terao, H. (1997). Development of an agricultural mobile robot using a geomagnetic direction sensor and image sensors. *Journal of Agricultural Engineering Research*, 67, 1–15.

Barawid, O. C. Jr., Mizushima, A., Ishii, K., and Noguchi, N. (2007). Development of an autonomous navigation system using two-dimensional laser scanner in an orchard application. *Biosystems Engineering*, 96(2), 139-149.

Kise, M. (2003), Development of General-Purpose Robot Tractor, *Memoirs of the Graduate School of Agriculture Hokkaido University*, 25(1), 1-60

Nagasaka, Y., Umeda, N., Kanetai, Y., Taniwaki, K., and Sasaki, Y. (2004). Autonomous guidance for rice transplanting using global positioning and gyroscopes. *Computers and Electronics in Agriculture*, 43(3): 223-234.

Kise M., Noguchi, N., Ishii, K. and Terao,H., (2001), Development of the agricultural tractor with an RTK-GPS and FOG. In Proc. Fourth IFAC symposium on intelligent autonomous vehicle, 103-108. Sapporo, Japan, 5-7 September.